Degeneracy in the emergence of spike-triggered average of hippocampal pyramidal neurons

Abha Jain and Rishikesh Narayanan

Cellular Neurophysiology Laboratory, Molecular Biophysics Unit,

Indian Institute of Science, Bangalore, India.

SUPPLEMENTARY INFORMATION

Supplementary Figure S1 2

Supplementary Figure S2 3

Supplementary Figure S3 4

Supplementary Figure S4 5

Supplementary Figure S5 6

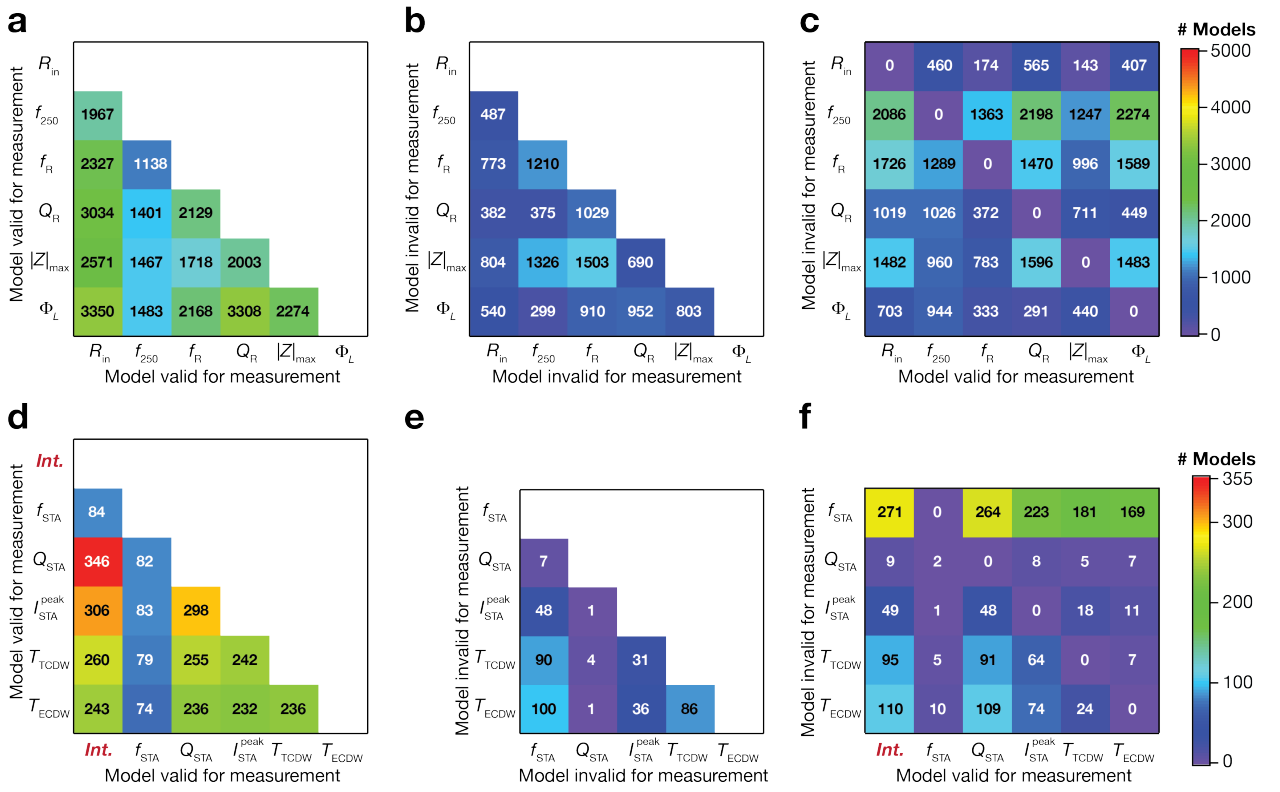

Supplementary Figure S1: Assessment of pair-wise dependencies of validity for measurements employed in this study. **(a)** Matrix representing pairwise count of models that were simultaneously valid for two of the 6 intrinsic physiological measurements (R_{in}, f_{250}, $|Z|_{max}$, f_R, Q_R, Φ_L). **(b)** Matrix representing pairwise count of models that are simultaneously invalid for two of the 6 intrinsic physiological measurements measurements. **(c)** Matrix representing pairwise count of models that are simultaneously valid for one intrinsic measurement and invalid for another of intrinsic measurements. **(a–c)** were performed for all the 5000 models. f_0, the spontaneous firing rate was identically zero for all 5000 models, and therefore is not depicted here. **(d–f)** Same as panels (a–c), but for the 355 models that satisfied validation criteria for the 7 intrinsic physiological measurements (represented as *Int*). The validation criteria for all the intrinsic and STA measurements are provided in Table 2.

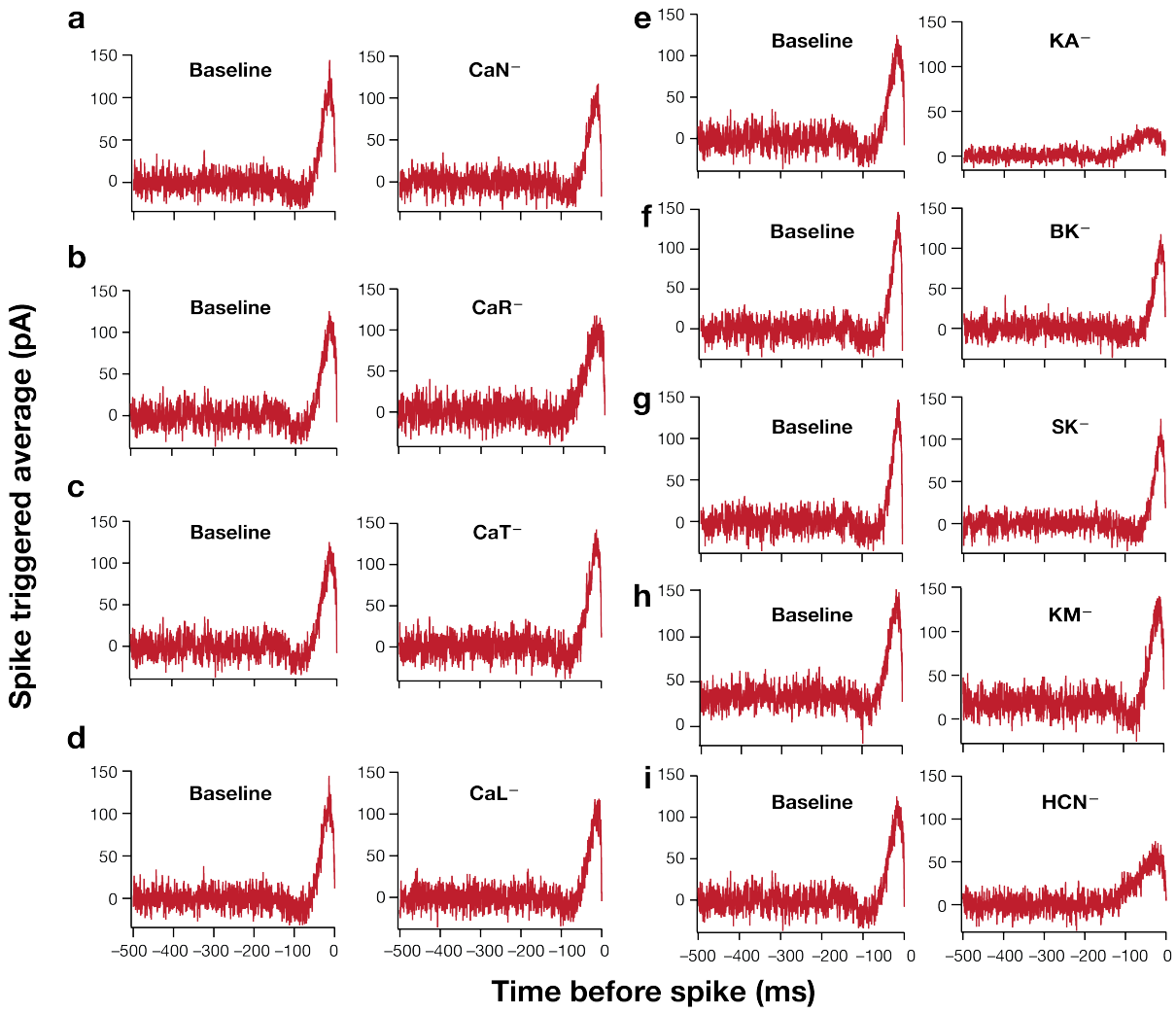

Supplementary Figure S2: A qualitative depiction of how knocking out specific ion channels affects a neuron's spike triggered average (STA). Each subpanel compares a neuron's STA under baseline conditions (left) with that of the same model lacking a specific ion channel (right); the ion channel that has been knocked out is indicated in each subpanel. For every graph, the *X*-axis is time before the generation of an action potential (in ms), while the *Y*-axis is STA current (in pA).

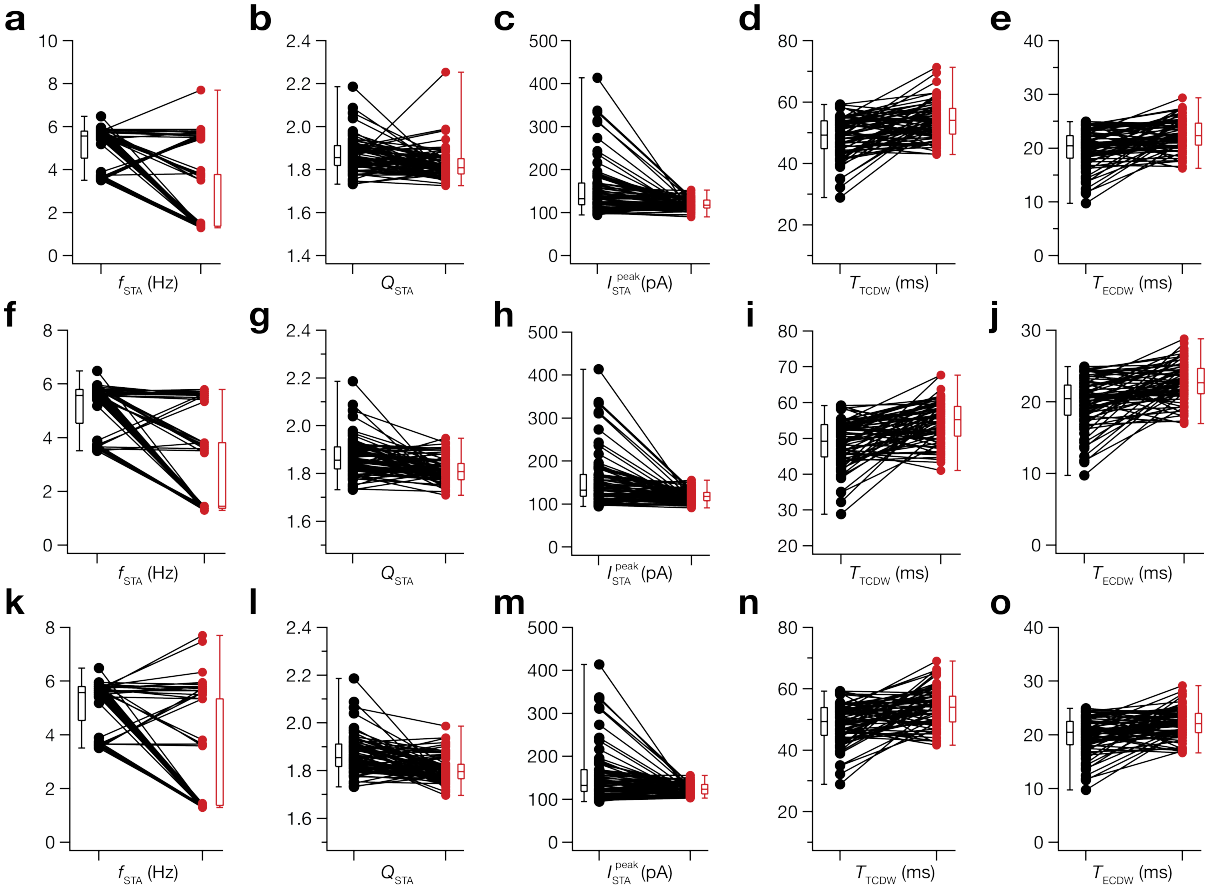

Supplementary Figure S3: Comparison of the five STA-based properties between the baseline models and the VKMs. In each subpanel, the black dots denote the values (for a given STA-based parameter) for the baseline models, while the corresponding red dots represent the same for the VKMs. The parameter under consideration is mentioned below each sub-panel. **(a–e)** are for the CaN knockout, **(f–j)** are for the CaR knockout, while **(k–o)** are for the CaL knockout.

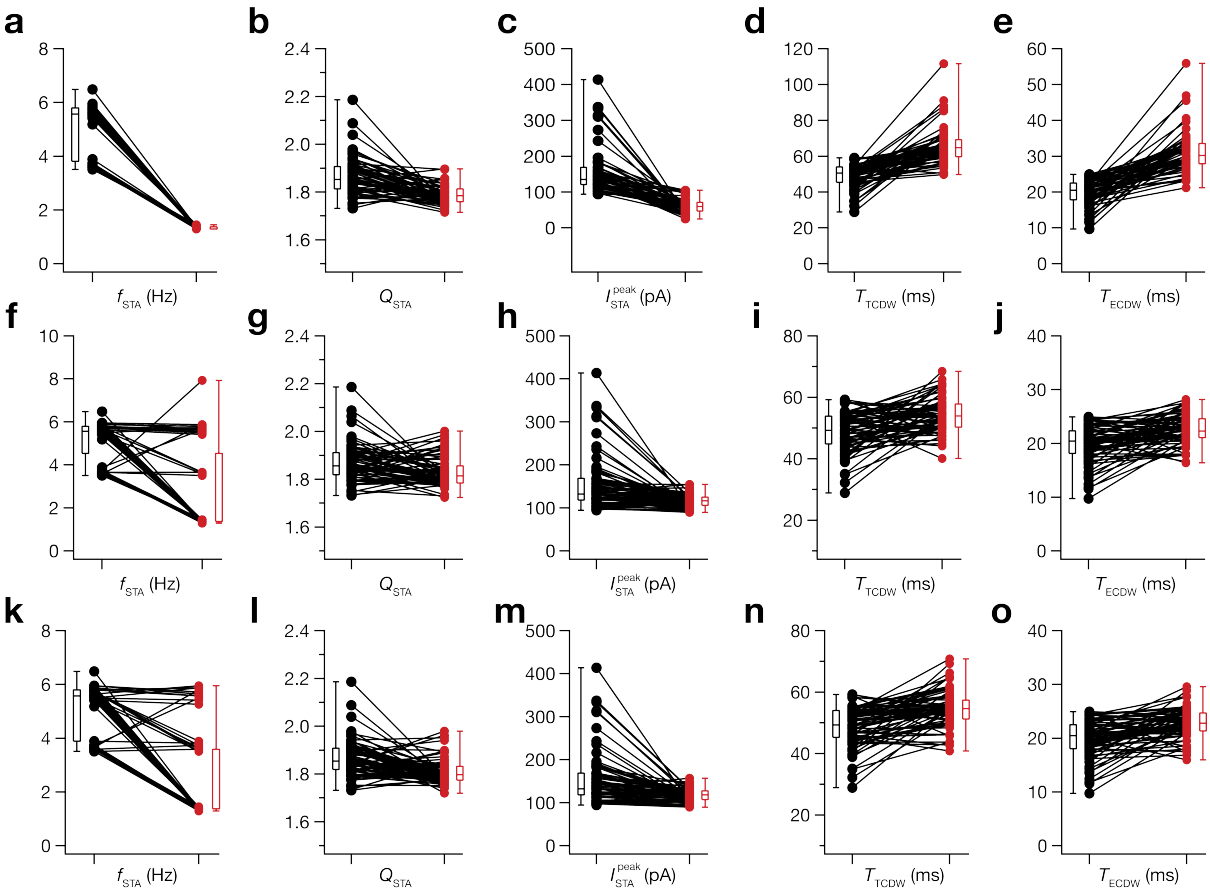

Supplementary Figure S4: Comparison of the five STA-based properties between the baseline models and the VKMs. In each subpanel, the black dots denote the values (for a given STA-based parameter) for the baseline models, while the corresponding red dots represent the same for the VKMs. The parameter under consideration is mentioned below each sub-panel. **(a–e)** are for the KA knockout, **(f–j)** are for the SK knockout, while **(k–o)** are for the BK knockout.

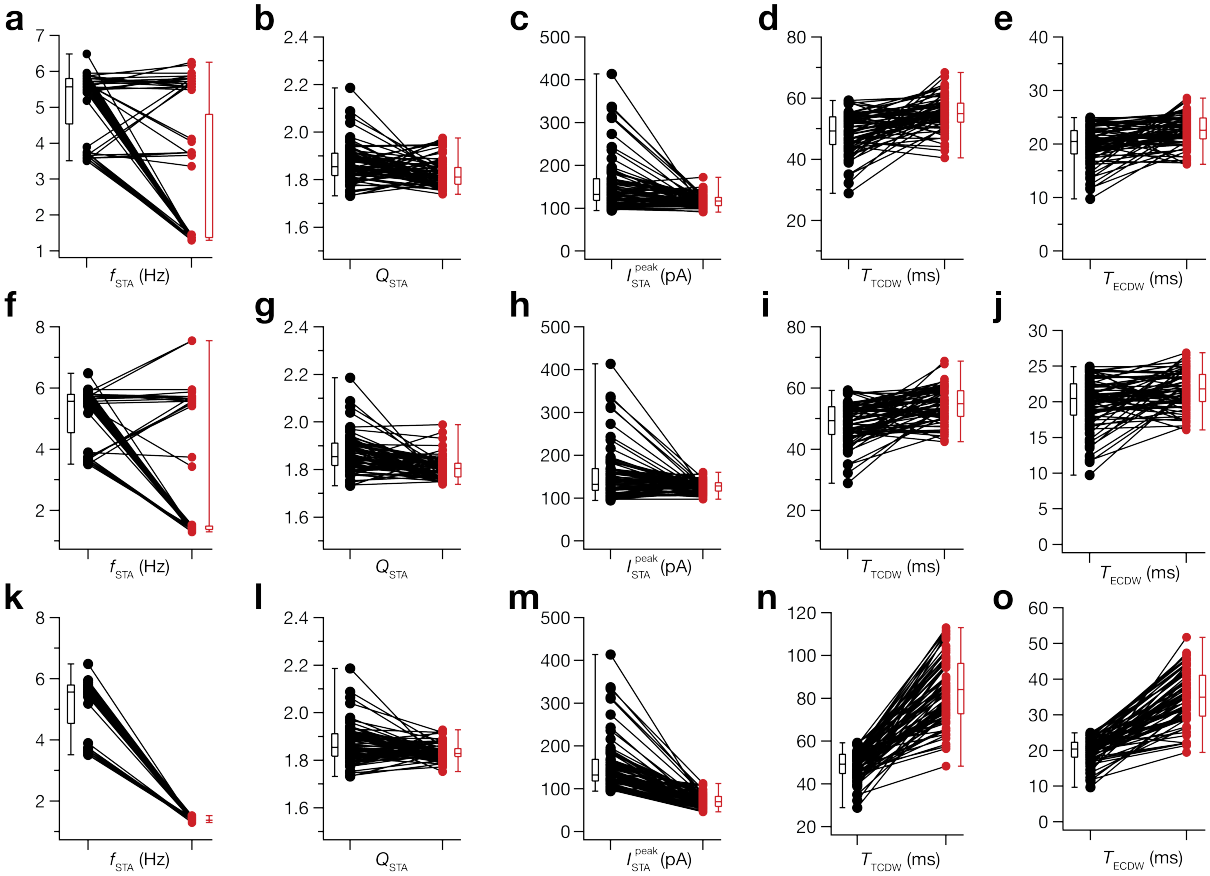

Supplementary Figure S5: Comparison of the five STA-based properties between the baseline models and the VKMs. In each subpanel, the black dots denote the values (for a given STA-based parameter) for the baseline models, while the corresponding red dots represent the same for the VKMs. The parameter under consideration is mentioned below each sub-panel. **(a–e)** are for the KM knockout, **(f–j)** are for the CaT knockout, while **(k–o)** are for the HCN knockout.